

# Gas dynamics of the active medium of a supersonic cw HF chemical laser

I A Fedorov, M A Rotinyan, A M Krivitskii

**Abstract.** Gas-dynamic characteristics of a 5-kW supersonic cw HF chemical laser with a nozzle array of size 25 cm  $\times$  2.8 cm and the nozzle–nozzle mixing scheme were experimentally studied. The distributions of Mach numbers, static pressure, total pressure behind the normal shock, and the loss of total pressure were measured in the flow of an active medium in wide ranges of variation of the flow rate of secondary fuel (hydrogen) and pressure in the atomic-fluorine generator. The energy parameters of the laser were found to be interrelated with the gas dynamics and the optical quality of the active laser medium.

## 1. Introduction

The active medium (AM) of a supersonic cw HF chemical laser represents a supersonic flow that is formed by initially separated small-scale jets of an oxidising gas (fluorine atoms) and a secondary fuel (hydrogen) flowing out from a nozzle array. The gas-dynamic phenomena taking place in this flow represent a kind of ‘background’ on which different processes are developed, such as the mixing of reagents used for chemical pumping, lasing, and relaxation of working molecules. This naturally draws attention to the characteristics of this background, which affects the output laser parameters. It is common to describe a supersonic gas flow by gas-dynamic characteristics such as total pressure  $p_{01}$  in the approach flow, the static flow pressure  $p_s$ , the Mach number  $M$  of the approach flow, and the loss in the total flow pressure.

What information on the AM can be obtained from the gas-dynamic measurements? First, the gas-dynamic characteristics of a flow at the output of a nozzle array affect the mixing of jets of an oxidising gas and a secondary fuel in a laser cavity and, therefore, the energy characteristics of the laser. Second, inhomogeneities of pressure (density) in the AM have a strong effect on its optical quality. Third, gas-dynamic characteristics of the medium leaving an optical cavity are important for the operation of the pressure recovery system during the evacuation of exhaust reaction products into the environment. Finally, the pressure distribution measured experimentally can be used as an objective criterion

for estimating the adequacy of mathematical models applied for the analysis of operation of cw HF chemical lasers.

It is evident that the gas dynamics of the AM is determined by the method of gas flow formation, which is specified by the design of a nozzle array. In Ref. [1], a detailed experimental study of gas-dynamic characteristics of a cw HF chemical laser using a nozzle array with radial expansion, which corresponds to the nozzle-injector scheme of reagent mixing, was performed. In this paper, we present the results of our study of a cw HF chemical laser using a nozzle array with the nozzle-nozzle scheme of reagent mixing. Our main goal was to study the effect of operation parameters of this laser on the gas dynamics of the AM flow and analyse its interrelation with the optical quality of the AM, the pressure recovery in the gas flow, and the energy parameters of the laser.

## 2. Experimental setup and the measurement technique

We studied an autonomous supersonic cw HF chemical laser, which was designed to operate at an output power of  $\sim 5$  kW. The laser had a nozzle array with the output section of size 25 cm  $\times$  2.8 cm. The nozzles feeding a secondary fuel ( $H_2$ ) and an oxidising gas (F) were arranged with a step of 7.5 mm. The active medium consisted of traditional reagents – gaseous deuterium, fluorine, helium, and hydrogen, which were taken in the molecular ratio  $D_2 : F_2 : He : H_2 = 1 : \alpha : \psi(\alpha - 1) : \alpha_2(\alpha - 1)$ . The laser was placed in a low-pressure chamber, which was used for separating the free gas flow escaping from the nozzle array from the environment.

We studied the dependence of gas-dynamic, optical, and energy characteristics of the AM on the secondary-fuel excess factor  $\alpha_2$ , which determines the hydrogen content, and the pressure  $p_c$  in the atomic-fluorine generator (AFG). We measured gas-dynamic characteristics of the AM, its length and optical quality, and the laser radiation power. In addition, we took motion pictures of the flow. The total pressure behind the normal shock and the static pressure were measured by the pneumometric method using uncooled probes (pressure samplers), which continuously moved along the axis of the optical cavity at a velocity of 2 mm  $s^{-1}$ .

The techniques used for gas-dynamic measurements and data processing are described in detail in Ref. [2]. Using the results of the measurements, we determined by the Rayleigh formula [3] the Mach numbers in the approach AM flow for the calculated adiabatic exponent. The length of the AM in the flow direction was estimated by the method of a double slit cavity [4], and its optical quality was controlled with a

I A Fedorov, M A Rotinyan, A M Krivitskii ‘Applied Chemistry’ Russian Scientific Centre, prosp. Dobrolyubova 14, 197198 St. Petersburg, Russia

Received 16 June, 2000

*Kvantovaya Elektronika* 30 (12) 1060–1064 (2000)

Translated by A N Kirkin

shear interferometer, [5] using the He–Ne laser radiation for probing the medium.

We measured the laser radiation power using a stable closed two-mirror cavity, which was formed by two uncooled spherical mirrors 9 cm in diameter with the 5-m radius of curvature. These mirrors were made of polished copper and simultaneously served as calorimeters. The technique used for power measurements is described in detail in Ref. [2]. Motion pictures of the AM flow were taken in the direction perpendicular to the axis of the optical cavity. We used a 1KSR-1M camera operating with a rate of 10 frames  $s^{-1}$ .

### 3. Experimental results

The effect of the secondary-fuel excess factor  $\alpha_2$  on the gas-dynamic characteristics of the cw HF chemical laser was studied at the optimum chemical fuel composition and the calculated (corresponding to a pressure of 5 Torr in the exit plane of the nozzle array) pressure in the AFG  $p_c^* = 0.09$  MPa (the corresponding total mass reagent flow was  $\sim 30$  g  $s^{-1}$ ). The optimum dimensionless parameters  $\alpha_{opt} = 1.7$  and  $\psi_{opt} = 10$  were determined by the method [6], and the coefficient  $\alpha_2$  was measured in the range between 5 and 23.

In each experiment, we varied the distance  $x_p$  from the exit plane of the nozzle array to the axis of mirrors-calorimeters and determined its optimum value ( $x_p^{opt} = 2.7 - 3.6$  cm) giving the maximum laser radiation power. The effect of pressure in the AFG on gas-dynamic characteristics of the cw HF chemical laser was studied for the optimum chemical fuel composition, the coefficient  $\alpha_2 = 9$  (close to the optimum value), and  $p_c$  varied in a range of  $0.7p_c^* \leq p_c \leq 1.7p_c^*$ .

#### 3.1. Pressure fields and Mach numbers in the active medium

To represent results in a convenient form, we used the coordinate system with the origin located at the centre of the exit plane of the nozzle array, the  $x$ -axis being directed along the flow, the  $y$ -axis being directed along the nozzles in the exit plane, and the  $z$ -axis being directed along the side edge of the array. The flow sections removed from the exit plane of the nozzle array in a range of distances 0.5–5 cm along the  $x$ -axis with a step of 0.5 cm were used as basis sections.

Using the profiles of total pressure  $p_{02}$  behind the normal shock and of static pressure  $p_s$  in the approach flow measured at three values of the coefficient  $\alpha_2$ , one can study in detail the gas dynamics of the AM flow. Some of these experimental profiles are presented in Figs 1a and 1b. In particular, one can clearly see in them the regions where pressure shocks take their origin. They govern the configuration of the profiles, especially at the initial stage of the flow adjacent to the exit plane of the nozzle array. One of the possible causes of the origin of pressure shocks is the difference of pressures at the output of nozzles used for the oxidising gas and the secondary fuel ( $p_{H_2} \neq p_F$ ). In this case, oblique shocks emerging from the edges of oxidiser nozzles and intersecting at a certain angle should be formed in the flow. The form of the  $p_{02}$  profiles measured in the section  $x = 0.5$  cm supports this assumption.

The configuration of the profiles measured downstream the flow is caused by the interaction of shock waves with one another, their reflection from the axes of symmetry of the jets, the viscosity, and the heat released in the exothermic chemical pump reaction  $F + H_2 \rightarrow HF(v) + H$ . The profiles are substantially nonuniform, and a strong nonuniformity is

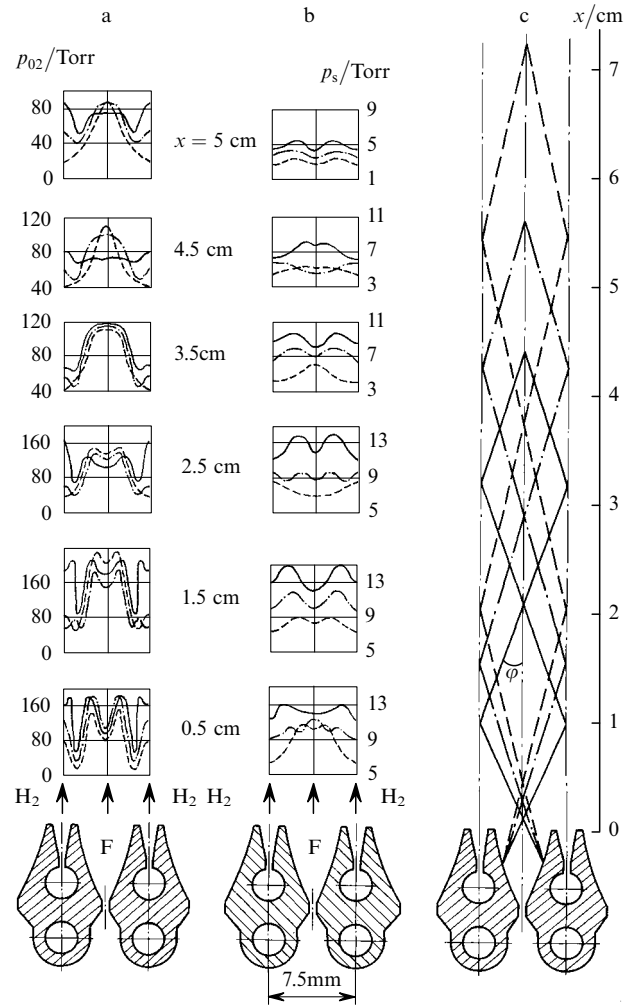


**Figure 1.** Experimental profiles of total pressure behind the normal shock (a) and the static pressure (b) measured at different distances  $x$  from the exit plane of the nozzle array for the secondary-fuel excess factors  $\alpha_2 = 5$  (dashed curves), 9 (dash-and-dot curves), and 23 (solid curves), and the corresponding approximate structure of shocks in the AM flow field (c).

persists throughout the active region ( $x \leq 7$  cm). Note that the degree of nonuniformity increases with increasing coefficient  $\alpha_2$ . This fact is associated with the intensification of mixing of reagent jets and is supported by the analysis of moving pictures of the overall pattern of the AM flow, according to which the conventional mixing length [2] decreases with increasing  $\alpha_2$ . This exerts an adverse effect on the optical quality of the AM. The increase in  $\alpha_2$  from 5 to 23 leads to the decrease in the Strehl ratio  $St$  from 0.72 to 0.45.

Using typical wakes of shock waves in the profiles of total pressure (Fig. 1a), we found their approximate structure, which is shown in Fig. 1c. As the coefficient of secondary-fuel excess increases, which is accompanied by an increase in the difference between  $p_{H_2}$  and  $p_F$ , the jet at the exit of the oxidiser nozzle becomes more and more ‘overexpanded’ with respect to the neighbouring jets of secondary fuel, and the oblique shock induced by their dynamic interaction becomes stronger. Because of this, the angle of inclination  $\phi$  of the shock front to the velocity vector of the approach flow of the oxidising gas increases by  $5^\circ$  (from  $17^\circ$  to  $22^\circ$ ) when  $\alpha_2$  is varied from 5 to 23. As the distance from the exit plane of the nozzle array is increased, the period of the rhomb-shaped shock structure increases, which is caused

by the expansion of the gas flow as a whole during its free outflow from the nozzle into the low-pressure chamber.

Fig. 2 presents the distributions of total and static pressures and Mach numbers along the AM flow for three characteristic flow directions: along the axes of oxidising-gas and secondary fuel nozzles and along their boundary (the mixing layer). The axial pressure distributions (Figs 2a, 2b, 2d, and 2e) have a periodic structure, which is formed due to the reflection of oblique shock waves from the symmetry axes of the jets. The positions of maxima and minima of static pressure in reagent jets at the initial flow stage are in anti-phase, which agrees well both with the overall flow pattern observed in moving pictures and with the calculations made using the mathematical model based on the full system of Navier–Stokes equations [7].

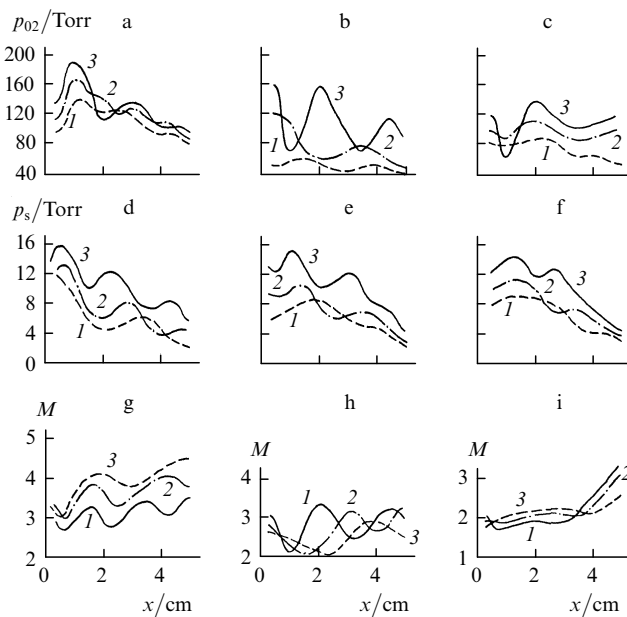


**Figure 2.** Longitudinal distributions of total pressure behind the normal shock (a–c), the static pressure (d–f), and Mach numbers (g–i) in the AM flow for secondary-fuel excess factors  $\alpha_2 = 5$  (1), 9 (2), and 23 (3), corresponding to the flow along the axes of oxidising-gas (a, d, g) and secondary-fuel (b, e, h) nozzles and along the mixing layer (c, f, i).

The static pressure  $p_s \sim 11$  Torr measured at the exist of the oxidising nozzle exceeds the value calculated by the isentropic relations by a factor of 1.5, which may be caused by two reasons, namely, the compression of the oxidising-gas jet in moving across the front of an oblique shock wave emerging from the nozzle and by the viscosity that leads to a decrease in the effective degree of the nozzle expansion. As the distance from the exit plane of the nozzle array is increased, one observes a decrease in the average static pressure. This effect is caused by the jet expansion into a free space of the low-pressure chamber and is observed till the levelling of pressures in the central part of the flow and in the environment. Our experiments showed that this process terminates at the distance  $x \sim 10$  cm from the exit plane of the nozzles. As the coefficient  $\alpha_2$  is increased, the total and the static pressures in the flow increase, and the maxima of their distributions shift toward the exit plane of the nozzle array because of the aforementioned increase in the angle  $\varphi$ .

The distribution of Mach numbers along the axes of reagent nozzles (Figs 2g and 2h) are also periodic because

of the reasons mentioned above. In the mixing layer (Fig. 2i), the Mach number has the value  $M = 2$  and weakly depends on the coefficient  $\alpha_2$ . However, at  $x > 3.5$  cm, the Mach number increases downstream. It is likely that in this region the acceleration of the flow due to its expansion as a whole prevails over slowing-down due to perturbations at shocks and the heat released in the exothermic physical and chemical transformations.

As  $\alpha_2$  is increased, the region of an intense increase in Mach number approaches the exit plane of the nozzle array, which indirectly confirms our assumption that the mixing of reagent jets is intensified. The Mach number  $M_1 = 3.5$  measured in the output section of the oxidising nozzle was found to be lower than the calculated value  $M_2 = 4.2$ . This difference may be explained by two reasons. First, because of the mismatch between pressures at the exit of secondary-fuel and oxidising-gas nozzles, the flow separation may take place in the latter (Fig. 1c). Second, the oxidising nozzles used in our laser have a radial shape (the profile of their supersonic region is formed by a circular arc). As the experimental study of the gas dynamics of such nozzles showed [8], they are characterised by an intense shock structure, which leads to a considerable loss in the total pressure and, therefore, a decrease in the Mach number.

The effect of pressure in the AFG on the gas-dynamic characteristics of the cw HF chemical laser predominantly manifests itself in the rate of levelling of inhomogeneities of the pressure fields in the AM flow and in the total pressure. The rate of inhomogeneity levelling decreases with increasing  $p_c$ . It is likely that this effect is caused by a decrease in the rate of reagent jet mixing with increasing  $p_c$ , which is confirmed by the results of processing of moving pictures. An increase in  $p_c$  causes a stronger increase in the total AM pressure than an increase in the coefficient  $\alpha_2$ .

### 3.2. Loss in the total pressure in the AM flow

It is common to characterise the loss in total pressure in the AM flow by the average recovery factor  $\bar{\sigma} = \bar{p}_{01}/p_c$ , where  $\bar{p}_{01}$  is the averaged total pressure in the approach AM flow, which is determined from the averaged (by integration over the period of the nozzle array  $0 \leq y \leq 7.5$  mm) profiles of pressures  $p_{02}$  and  $p_s$ . As follows from Fig. 3a, the losses in total pressure in the gas-dynamic laser channel are rather high and depend on the secondary-fuel excess factor. As the latter is increased, the total pressure in the AM flow increases due to an increase in pressure in hydrogen jets. As  $\alpha_2$  is increased from 5 to 23, the coefficient  $\bar{\sigma}$  near the far boundary of the lasing region ( $x \sim 5$  cm) increases by a factor of about 1.5.

It is somewhat unexpected that the pressure recovery factor decreased with increasing  $p_c$  (Fig. 3b). In particular, at  $p_c = 0.15$  MPa (curve 6), the coefficient  $\bar{\sigma}$  is lower by a factor of 1.4 than its value at the calculated pressure  $p_c^* = 0.09$  MPa (curve 5), and when  $p_c = 0.06$  MPa (curve 4), it is higher by a factor of 1.25. This may be caused by the strengthening of combustion-initiated shocks with increasing pressure in the optical cavity.

### 3.3. Gas dynamics of the active medium and the laser energy characteristics

The dependences of the radiation power  $N$  of the HF laser and its specific output power  $N_\Sigma$  on the secondary-fuel excess factor are presented in Fig. 4a. In the region  $5 \leq \alpha_2 \leq 23$  studied by us, these dependences are rather weak. The opti-

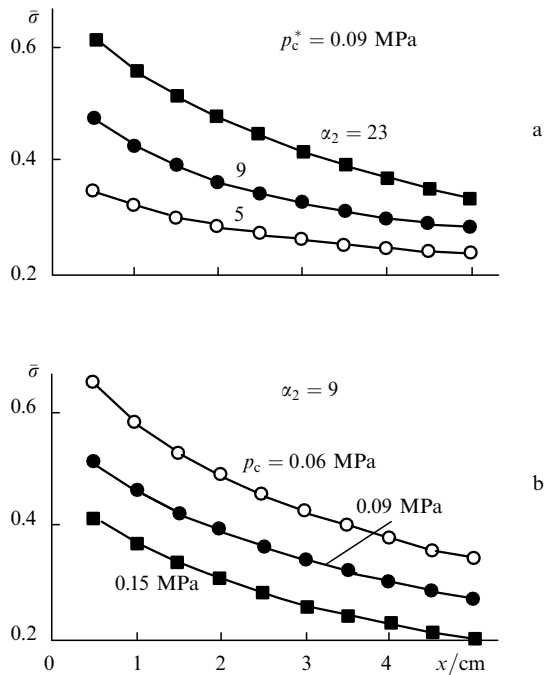


**Figure 3.** Longitudinal distributions of the averaged pressure recovery factor in the AM flow  $\bar{\sigma}$  for  $p_c^* = 0.09$  MPa,  $\alpha_2 = 5, 9$  and  $23$  (a) and at  $\alpha_2 = 9$ ,  $p_c = 0.06, 0.09$ , and  $0.15$  MPa (b).

imum value is  $\alpha_2^{\text{opt}} = 12 - 13$ . However, one may considerably decrease this value without a noticeable decrease in laser energy characteristics. In particular, the twofold decrease in the hydrogen flow rate with respect to the optimum value ( $\alpha_2^{\text{opt}} = 12$ ) causes a decrease in the radiation power only by  $\sim 10\%$ . On the other hand, as  $\alpha_2$  is decreased, the degree of inhomogeneity of the field of total and static pressures in the flow also decreases (Figs 1a and 1b), which offers promise for an improvement of the optical quality of the AM. Therefore, the regimes with low  $\alpha_2$  are preferential for obtaining high energy parameters of radiation in the far-field zone. However, a decrease in  $\alpha_2$  reduces the efficiency of recovery of the total pressure in the AM flow, i.e., causes a decrease in the coefficient  $\bar{\sigma}$  (Fig. 3a).

As for the pressure in the AFG, our experiments showed that its decrease is accompanied by the improvement in both energy (an increase in the specific output power, Fig. 4b) and gas-dynamic (a decrease in the loss in total pressure, Fig. 3b) laser characteristics. In this situation, the obtaining of maximum radiation power  $N^{\text{max}}$  may be used as one of the criteria for the choice of optimum values of  $p_c$  and  $\alpha_2$ . Another important parameter is the product of the normalised radiation power by the Strehl ratio ( $N/N^{\text{max}}$ )Sh. This generalised criterion, which was proposed in [9], enables one to determine the regions of allowable changes in operation parameters of the HF laser at which the combination of rather high laser output parameters with a good optical quality of the AM is realised.

### 3.4. The effect of pressure in reagent jets on the gas dynamics of the active medium

As noted above, the ratio  $p_{\text{H}_2}/p_{\text{F}}$  of pressures in the jets of secondary fuel and oxidising gas is one of the parameters determining the gas-dynamic pattern of the flow in the optical cavity. This raises the question of the influence of this parameter on the energy characteristics of the given laser.

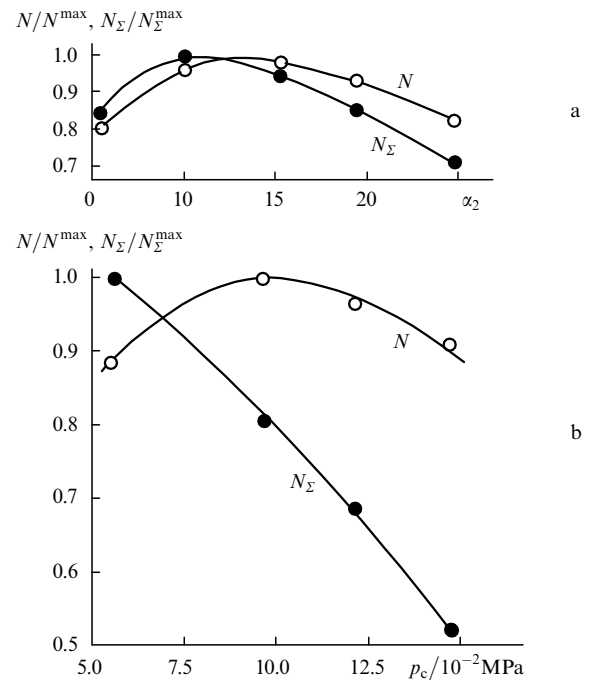


**Figure 4.** Dependences of the radiation power  $N$  and the specific output energy  $N_\Sigma$  of the cw HF chemical laser on the secondary-fuel excess factor  $\alpha_2$  (a) and the pressure in the AFG  $p_c$  (b).

In our experiments, we realised the conditions with  $0.4 \leq p_{\text{H}_2}/p_{\text{F}} \leq 1.5$ . The ratio  $p_{\text{H}_2}/p_{\text{F}} = 0.8$  was optimum for obtaining the maximum radiation power. It corresponded to the situation in which the static pressure at the exit of the oxidising-gas nozzle was somewhat higher than the pressure at the exit of the secondary-fuel nozzle. This result agrees well with the conclusions of the computational theoretical analysis [10].

In summary, on the basis of our study, we formulated the criteria for optimising the performance of the supersonic cw HF chemical laser.

**Acknowledgements.** The authors thank A V Veselovskii, S V Konkin, and V L Moshkov for their participation in the measurements and help in the experiments.

### References

1. Rebene V K, Rotinyan M A, Fedorov I A, et al *Kvantovaya Elektron.* **24** 880 (1997) [*Quantum Electron.* **27** 855 (1997)]
2. Fedorov I A *Nepreryvnye khimicheskie lazery na rabochikh molekulakh fluoristogo vodoroda i fluoristogo deiteriya* (CW Chemical Lasers Operating on Hydrogen Fluoride and Deuterium Fluoride Molecules) (St. Petersburg: Izd. Baltic State Technical University, 1994) Vol. 2
3. Petunin A N *Metody i tekhnika izmerenii parametrov gazovogo potoka* (Methods and Instruments for the Measurement of Gas Flow Parameters) (Moscow: Mashinostroenie, 1972)
4. Galaev I I, Konkin S V, Rebene V K, Fedorov I A *Prib. Tekh. Eksp.* No. 1 122 (1997)
5. Bashkin A S, Boreisho A S, Lobachev V V, et al. *Kvantovaya Elektron.* **23** 428 (1996) [*Quantum Electron.* **26** 418 (1996)]
6. Rebene V K, Rotinyan M A, Fedorov I A, et al. *Kvantovaya Elektron.* **23** 707 (1996) [*Quantum Electron.* **26** 688 (1996)]
7. Shur M *Proceedings of the International Conference on Numerical Methods in Laminar and Turbulent Flows*, Stanford, USA, 1991, Vol. 7, pt. 2, 1526

8. Ktalkherman M G, Ma'kov V M, Ruban N A in *Issledovanie rabocheho protsessa gazodinamicheskikh i khimicheskikh lazerov* (The Study of the Working Process in Gas-Dynamic and Chemical Lasers) (Novosibirsk: Izd. ITPM, Siberian Division of the Russian Academy of Sciences, 1979) p. 3
9. Lobachev V V, Fedorov I A *Opt. Spektrosk.* **82** 153 (1997) [*Opt. Spectrosc.* **82** 138 (1997)]
10. Rotinian M., Shur M., Strelets M. *Proc. XXV Intern. Symp. on Combustion* (Irvine, USA, 1994) p.13